Heliyon 10 (2024) e27915

Contents lists available at ScienceDirect

Heliyon

journal homepage: www.cell.com/heliyon

Research article

Highly efficient ceramic membrane synthesized from sugar scum and fly ash as sustainable precursors for dyes removal

Y. El maguana [a,*], R. Chikri [a], K. Elataoui [a], H. Ait Said [b], M. Benchanaa [a], N. Elhadiri [a]

[a] Laboratory of materials science and process optimization (SCIMATOP), Faculty of Science Semlalia, Cadi Ayyad University, B.P. 2390, Marrakech, Morocco

[b] High Throughput Multidisciplinary Research Laboratory (HTMR), Mohammed VI Polytechnic University (UM6P) Benguerir 43150, Morocco

ARTICLE INFO

Keywords:
Ceramic membrane
Sugar scum
Fly ash
Anorthite
Experimental design

ABSTRACT

Recycling solid industrial wastes into valuable materials is always the priority solution in waste management. In this perspective, sugar scum and fly ash were used to produce an effective low-cost porous ceramic membrane. The impacts of the sintering temperature, amount of sugar scum, and sintering time on the properties of the prepared ceramic membrane were investigated and optimized using experimental design. A simultaneous rise in both the sintering temperature and the amount of sugar scum leads to a notable increase in porosity. Moreover, the simultaneous increase or decrease in the time and the amount of sugar scum causes a significant decrease in the compressive strength. The optimal conditions have been determined as a sintering temperature of 1197 °C, a sugar scum amount of 12.06 %, and a sintering time of 253 min. Under these conditions, the density, porosity, and compressive strength were found to be 2.16 g/cm^3, 34.66 %, and 28.24 MPa, respectively. In addition, the obtained ceramic membrane has a water permeability of 2356.68 L/h m^2 bar, a pore size in the range 0–4.5 μm, and excellent chemical resistance in both acidic and basic media. Finally, the performance of the prepared ceramic membrane was evaluated by the filtration of methylene blue. The results indicate that sugar scum and fly ash are suitable precursors to manufacture an effective ceramic membrane for the treatment of wastewater.

1. Introduction

The growing population and the bettering economic conditions have resulted in noteworthy challenges, such as a continual rise in industrial waste production. These wastes present a considerable environmental challenge, potentially causing environmental harm and adverse impacts on the health of humans and animals if not appropriately disposed of into the environment [1]. The management of waste has become a priority in environmental policies. For this reason, industries are actively seeking durable and practical solutions to reduce the substantial quantities of waste through the adoption of innovative approaches that align with the seventeen sustainable development goals. Therefore, researchers have become increasingly interested in the management of waste, which can be valorized and employed for diverse applications. Consequently, solid wastes are utilized to prepare various value-added materials, such as adsorbents [2], ceramic materials [3], membranes [4], composting fertilizer [5], energy [6], etc.

* Corresponding author.
E-mail address: youssefelmaguana@gmail.com (Y. El maguana).

https://doi.org/10.1016/j.heliyon.2024.e27915
Received 13 December 2023; Received in revised form 27 February 2024; Accepted 8 March 2024
Available online 9 March 2024

Recently, ceramic membranes have undergone rapid evolution due to their remarkable characteristics, including high mechanical strength and chemical stability, excellent thermal resistance, minimal pollution, corrosion resistance, and long-lasting performance [7]. They are now widely recognized as a reliable and economic solution, finding extensive use in many industrial applications and processes, for example, removal of pollutants [8–10], biotechnology and medical uses [11], catalysis [12], food industry, petrochemistry, and desalination [13–15].

Commercial ceramic membranes made from metal oxides like silica (SiO_2) [16], titania (TiO_2) [17], zirconia (ZrO_2) [18], and alumina (Al_2O_3) [19], or a mixture of these oxides, are quite limited in their applications due to their high cost. To overcome this limitation, scientific research has been focused on producing ceramic membranes using low-cost alternative starting materials [20,21]. Previous studies have reported the utilization of various abundant and inexpensive solid waste materials and geomaterials in the preparation of ceramic membranes such as kaolin [22], phosphates [23], natural perlite [21], natural magnesite [24], bentonite [25], pozzolan [26], fly ashes [27], etc. The use of industrial solid wastes as raw precursors in the manufacture of ceramic membranes helps decrease solid waste, produce low-cost materials of high value, and protect the environment.

Fly ash and sugar scum are produced as by-products of coal combustion and sugar-refining process, respectively. These wastes have led to significant environmental problems related to their disposal on land. The primary chemical constituents of fly ash are Al_2O_3 (28.4 wt%) and SiO_2 (56.6 wt%) [28], while sugar scum contains a higher percentage of CaO (46.38 wt%) [1]. The current study aims to investigate the potential utilization of these two wastes as low-cost precursors for the preparation of an economical and efficient anorthite-based ceramic membrane (anorthite, CaO; Al_2O_3; $2SiO_2$) for dye removal from aqueous solutions. Because of its outstanding characteristics, such as high thermal shock resistance, low thermal expansion coefficient, and small dielectric constant, the anorthite phase shows promise as a candidate for ceramic membrane preparation. In addition, the release of CO_2 from the sugar scum during sintering suggests that it could potentially function as a pore-forming agent, resulting in the production of a porous ceramic membrane. To the best of our knowledge, the use of fly ash and sugar scum for manufacturing an anorthite-based ceramic membrane to remove dyes from aqueous solutions has not been studied.

To achieve this objective, the Doehlert experimental design was employed to investigate the impacts of sintering temperature, amount of sugar scum, and sintering time on the properties of ceramic membranes, including the density, porosity, and compressive strength. The optimal ceramic membrane was characterized using various methods and was subsequently tested for its effectiveness in removing methylene blue from an aqueous solution.

2. Materials and methods

2.1. Materials

In this study, the starting precursors used for the preparation of low-cost membranes were fly ash and sugar scum. Coal fly ash was obtained from a thermal power plant in Jorf Lasfar El-Jadida, Morocco, while sugar scum was procured from a discharge of a sugar factory situated in Beni Mellal, Morocco. These materials were dried at 110 °C for 24 h, crushed, and sieved to obtain particle sizes less than 100 μm. Methylene blue (MB) used for the filtration test in the present study was supplied by Merck. All solutions were prepared with deionized water.

2.2. Preparation of ceramic membrane

The flat ceramic membranes, 20 mm in diameter and 2 mm in thickness, were formed using the dry pressing technique by mixing fly ash and sugar scum. The membrane powders were prepared by modifying the amount of sugar scum in the range of 0–20 wt %. Thereafter, the homogenized mixture was uniaxially pressed into the cylindrical mold of 20 mm in diameter and pressed under 2 tonnes for 10 min using a uniaxial hydraulic press to prepare a flat ceramic membrane. The resulting ceramic membrane was thermally treated in a tubular furnace (Carbolite Ltd, UK) at various temperatures ranging from 1000 to 1200 °C for varying durations ranging from 2 h to 6 h. The heating rate for the thermal treatment was set at 5 °C/min. After cooling to ambient temperature, the sintered membranes were preserved for subsequent experimental applications.

2.3. Material characterization

The chemical composition of fly ash and sugar scum was determined using ICP-AES. The identification of phases was conducted using X-ray diffraction analysis using a Bruker Advanced D8 diffractometer operating with a copper anticathode ($\lambda K\alpha = 1.54060$ Å) to determine the different phases existing in the examined materials. Scanning electron microscopy coupled with energy dispersive X-ray spectroscopy (SEM/EDX) was utilized to analyze the morphological features of raw materials and the elaborated ceramic membrane as well as to identify its elemental composition utilizing the Tescan Vega3 instrument with an accelerating voltage of 20 kV. The functional groups were identified by Fourier Transformed Infrared (FTIR) spectroscopy on a Bruker Vertex 70 spectrophotometer ranging from 4000 to 400 cm^{-1} with a resolution of 4 cm^{-1}.

The compressive strength of the prepared samples was determined with an Instron 3369 apparatus under a load of 50 kN and a loading speed of 0.1 mm/min. The ceramic membranes' density was determined using an electronic densimeter H300–S. The water absorption (WA) was calculated using Eq. (1) [29].

$$WA\% = \frac{m - m_0}{m_0} \times 100 \quad \text{Eq.1}$$

Where m_0 and m represent the membrane weights before and after immersing in boiling water for 2 h.

The corrosion resistance capacity of the ceramic membrane prepared under optimal conditions was tested in very harsh environments such as acidic and basic solutions. First, the ceramic membrane was dipped in HCl (0.1 M) and NaOH (0.1 M) solutions during one week [4]. Second, the treated sample was washed to eliminate any deposited precipitate on the surface of the membranes and then dried at 110 °C overnight. Finally, the untreated and treated membrane weights were used for calculating the corrosion resistance using Eq. (2).

$$\text{Weight loss} = \frac{m_i - m_f}{m_i} \times 100 \quad \text{Eq. 2}$$

Where m_i and m_f are the weights of membranes before and after treatment, respectively.

The permeability of the optimal ceramic membrane was experimentally measured by filtration of water at ambient temperature (25 ± 2 °C) at different pressures ranging from 0 to 1 bar. The permeate flux (J_w, L/h m^2) was determined using Eq. (3), and the water permeability (L_p, L/h.m^2.bar) was calculated from the variation of the water flux against the transmembrane pressure (ΔP) according to Darcy's low given in Eq. (4).

$$J_w = \frac{V}{A.t} \quad \text{Eq. 3}$$

$$L_p = \frac{Jw}{\triangle P} \quad \text{Eq. 4}$$

Where V (L) is the volume of permeate, t (h) is the filtration time, A (m^2) is the effective membrane area of the ceramic membrane, and ΔP (bar) is the transmembrane pressure.

2.4. Filtration experiment

The efficacy of the optimum ceramic membrane was assessed through the filtration of a MB solution (C_0 = 50 mg/L). The filtration test was performed under constant transmembrane pressure of 1 bar for 2 h and at ambient temperature (25 ± 2 °C) using the experimental setup shown in Fig. 1. To evaluate the ceramic membrane's separation efficiency, the removal percentage R (%) of MB was calculated using Eq. (5).

$$R = \frac{C_i - C_p}{C_i} \times 100 \quad \text{Eq. 5}$$

Where C_i (mg/L) and C_p (mg/L) are the initial and the permeate concentration of MB, respectively.

The MB concentration in both the feed and permeate was measured using the spectrophotometric method (UV–3100PC Spectrophotometer) at a wavelength of 664 nm [30]. The calibration curves for MB dye (correlation coefficient $R^2 \sim 0.99$) were generated within the concentration range of 0–7 mg/L, and the extinction coefficient was determined to be 0.202 L/mg.cm.

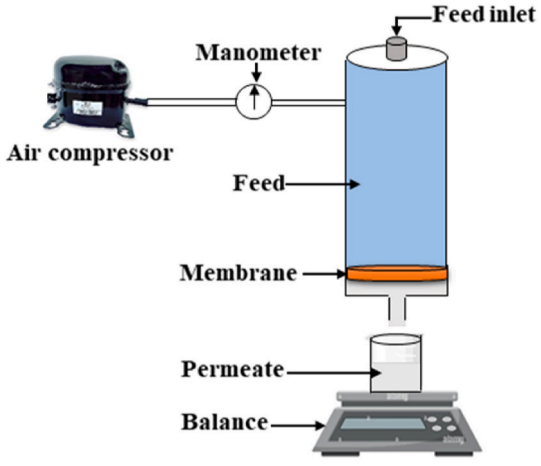

Fig. 1. Experimental setup for filtration test.

2.5. Experimental design

This study employed the experimental design to optimize the sintering temperature (T), the amount of sugar scum (τ), and the sintering time (t) in the experimental domains presented in Table 1. The examined responses were the density (Y_1, g/cm^3), the porosity (Y_2, %), and the compressive strength (Y_3, MPa). The three factors (T, τ, and t) were related to the responses by the model given in Eq. (6).

$$Y = b_0 + b_1X_1 + b_2X_2 + b_3X_3 + b_{11}X_1^2 + b_{22}X_2^2 + b_{33}X_3^2 + b_{12}X_1X_2 + b_{13}X_1X_3 + b_{23}X_2X_3 \quad \text{Eq. 6}$$

Where, Y is the response, X_1, X_2, and X_3 are the coded variables corresponding to T, **τ**, and t, respectively. b_0 is a constant, while b_1, b_2, and b_3 represent the main effects of T, *τ*, and t, respectively. b_{12} is the interaction effect between T and **τ**, b_{13} is the interaction effect between T and t, and b_{23} is the interaction effect between **τ** and t. b_{11}, b_{22}, and b_{33} can be considered as a curve shape parameter.

In this work, the Doehlert matrix was applied to create the experimental design, to calculate the coefficients of the model, and also to interpret the results using the obtained graphics of the studied responses.

3. Results and discussion

3.1. Characterization of raw materials

The chemical compositions of fly ash and sugar scum determined by (ICP-AES) are summarized in Table 2. Fly ash is mainly composed of SiO_2 (58.58 wt %) and Al_2O_3 (28.74 wt %), representing readily available Si and Al sources, while sugar scum contains a higher percentage of CaO (46.38 wt%). The XRD patterns of fly ash and sugar scum are depicted in Fig. 2a. The results clearly elucidate that the primary crystal phases found in fly ash are mullite (JCPDS 79–1454) and quartz (JCPDS 65–0466). The presence of calcium carbonate as the main phase in the sugar scum was confirmed by matching its XRD peaks with those in the JCPDS 01-086-2339 database. Fig. 2b corresponds to the FTIR spectrums of fly ash and sugar scum. For the fly ash spectrum, the bands observed at 458, 558, and 791 cm^{-1} were attributed to asymmetric stretching vibrations of Si–*O*–Si and Si–*O*–Al [31]. The band appearing at 711, 873, 1074, and 2516 cm^{-1}, in the FTIR spectra of sugar scum, were assigned to the calcium carbonate [32]. The minor-intensity band at 1632 cm^{-1} was attributed to the bending vibrations of water molecules strongly adsorbed [1]. The band observed at 3444 cm^{-1} was assigned to the stretching vibrations of O–H in hydroxyl groups. FTIR analysis also validated that the mullite, quartz, and calcium carbonate are the main phases in the fly ash and sugar scum, and therefore they are suitable precursors for use as raw materials for the manufacturing of anorthite-based ceramic membranes.

Fig. 3 shows SEM micrographs of sugar scum and fly ash. The sugar scum shows a porous like-morphology (Fig. 3a). The morphology of fly ash revealed spherical particles with irregular shapes (Fig. 3b). The elemental analysis results obtained through EDX are shown in Fig. 3, indicating that these precursors contain significant percentages of aluminum, silica, and calcium, and consequently they can be utilized as raw materials to prepare ceramic membranes based on anorthite.

3.2. Optimization of the operating conditions

Table 3 presents the experimental design of Doehlert and the experimental results of the physical properties of the prepared ceramic membranes. The center of the experimental domain was replicated three times to reduce experimental errors and assess the reproducibility of the results. The analysis of variance (ANOVA) was employed to verify the accuracy and validity of the utilized model. Estimated coefficients for the density, compressive strength, and porosity are listed in Table 4. To interpret the results, Nemrod software was utilized to depict isoresponse curves, representing the surfaces of responses in the experimental intervals for the sintering temperature, the amount of sugar scum, and the sintering time. Fig. 4 illustrates the significant interactions (isoresponse curves and three-dimensional plots) between those variables for the density, the porosity, and the compressive strength.

3.2.1. Influence of variables on the density (Y_1)

The ceramic membranes' density, as shown in Table 3, ranges from 2.05 to 2.16 g/cm^3. The relationship between the density (Y_1) and the coded variables associated with the temperature of sintering, the amount of sugar scum, and the sintering time can be expressed as follows (Eq. (7)):

$$Y_1 = 2.11 + 0.031X_1 + 0.022X_2 + 0.014X_3 + 0.01X_1^2 + 0.007X_2^2 - 0.002X_3^2 - 0.075X_1X_2 + 0.014X_1X_3 + 0.034X_2X_3 \quad \text{Eq. 7}$$

It can be deduced from the coefficients' values, given in Table 4, that the temperature of sintering ($b_1 = 0.031$) has a positive impact

Table 1
Experimental intervals for the Doehlert design.

Factors	Symbol	Experimental domain
Sintering temperature (°C)	T	1000–1200
Amount of sugar scum (%)	τ	0–20
Sintering time (min)	t	120–360

Table 2
Chemical compositions (wt%) of the studied raw materials.

Oxides	SiO_2	Al_2O_3	Fe_2O_3	CaO	MgO	MnO	P_2O_5	SO_3
Fly ash (%)	58.58	28.74	5.36	0.95	0.18	0.01	0.4	0.13
Sugar scum (%)	0.59	<0.10	0.1	46.38	1.38	<0.01	1.19	0.67

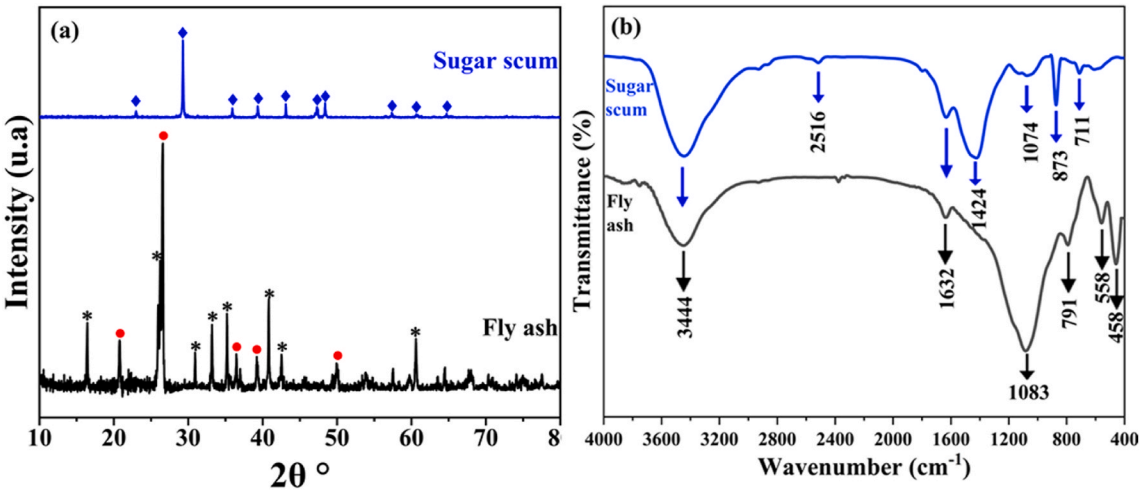

Fig. 2. (a) XRD patterns and (b) FTIR spectra of fly ash and sugar scum: ♦: calcium carbonate, ●: quartz, ✻ mullite.

and is the most influential factor on the density. Furthermore, one significant interaction exists between the sintering temperature and the amount of sugar scum ($b_{12} = -0.075$). The acquired model was employed to visually depict this interaction, as shown in Fig. 4a. The increase in the temperature of sintering from 1000 to 1200 °C for an amount of sugar scum less than 10 % leads to a substantial density increase, possibly resulting from a decrease in the ceramic membrane porosity. The higher temperature permits the consolidation of the matrix through the formation and development of the melt. Consequently, the ceramic membrane density increases. Furthermore, it can also be noticed that as the sugar scum amount increases from 0 to 20 %, there is a corresponding rise in the density at sintering temperatures ranging from 1000 to 1100 °C.

3.2.2. *Influence of variables on the porosity (Y_2)*

The porosity of the manufactured ceramic membranes, as presented in Table 3, ranges from 25.82 to 41.75 %. The variation of the porosity (Y_2) in the experimental intervals of the temperature, the amount of sugar scum, and the sintering time can be represented using Eq. (8).

$$Y_2 = 35.537\text{-}2.206X_1 + 5.324X_2\text{-}0.171X_3\text{-}0.217X_1^2\text{-}0.467X_2^2\text{-}0.659X_3^2 + 7.858X_1X_2\text{-}5.154X_1X_3\text{-}0.612X_2X_3 \quad \text{Eq. 8}$$

The values of coefficients, given in Table 4, showed that the more influential factor on the porosity is the amount of sugar scum ($b_2 = 5.324$) with a positive effect. Furthermore, a noteworthy interaction is observed between the temperature of sintering and the amount of sugar scum ($b_{12} = 7.858$). The resulting model was utilized to visually illustrate this interaction, as presented in Fig. 4b. The analysis of this interaction reveals that the simultaneous rise in the temperature and the amount of sugar scum leads to a significant increase in porosity. The presence of numerous pores in the obtained membranes results from carbonate decomposition and the liberation of carbon dioxide (CO_2). Also, the development of porosity can be ascribed to the presence of the gehlenite phase, renowned for its inherent ability to self-generate pores [33].

3.2.3. *Influence of variables on the compressive strength (Y_3)*

The compressive strength of the manufactured ceramic membranes, provided in Table 3, ranges between 3.19 and 37.54 MPa. The variation of the compressive strength (Y_3) as a function of the temperature of sintering, the amount of sugar scum, and the sintering time can be described by Eq. (9).

$$Y_3 = 11.967 + 10.01X_1\text{-}2.06X_2 + 5.381X_3 + 8.553X_1^2\text{-}8.403X_2^2\text{-}2.177X_3^2\text{-}2.511X_1X_2 + 6.932X_1X_3\text{-}14.724X_2X_3 \quad \text{Eq. 9}$$

As seen from the calculated coefficients' values, summarized in Table 4, the compressive strength is influenced by the temperature of sintering ($b_1 = 10.01$) and the sintering time ($b_3 = 5.381$) with a positive effect. In addition, the results indicate a significant interaction between the amount of sugar scum and sintering time ($b_{23} = -14.724$), the simultaneous increase or decrease in the time

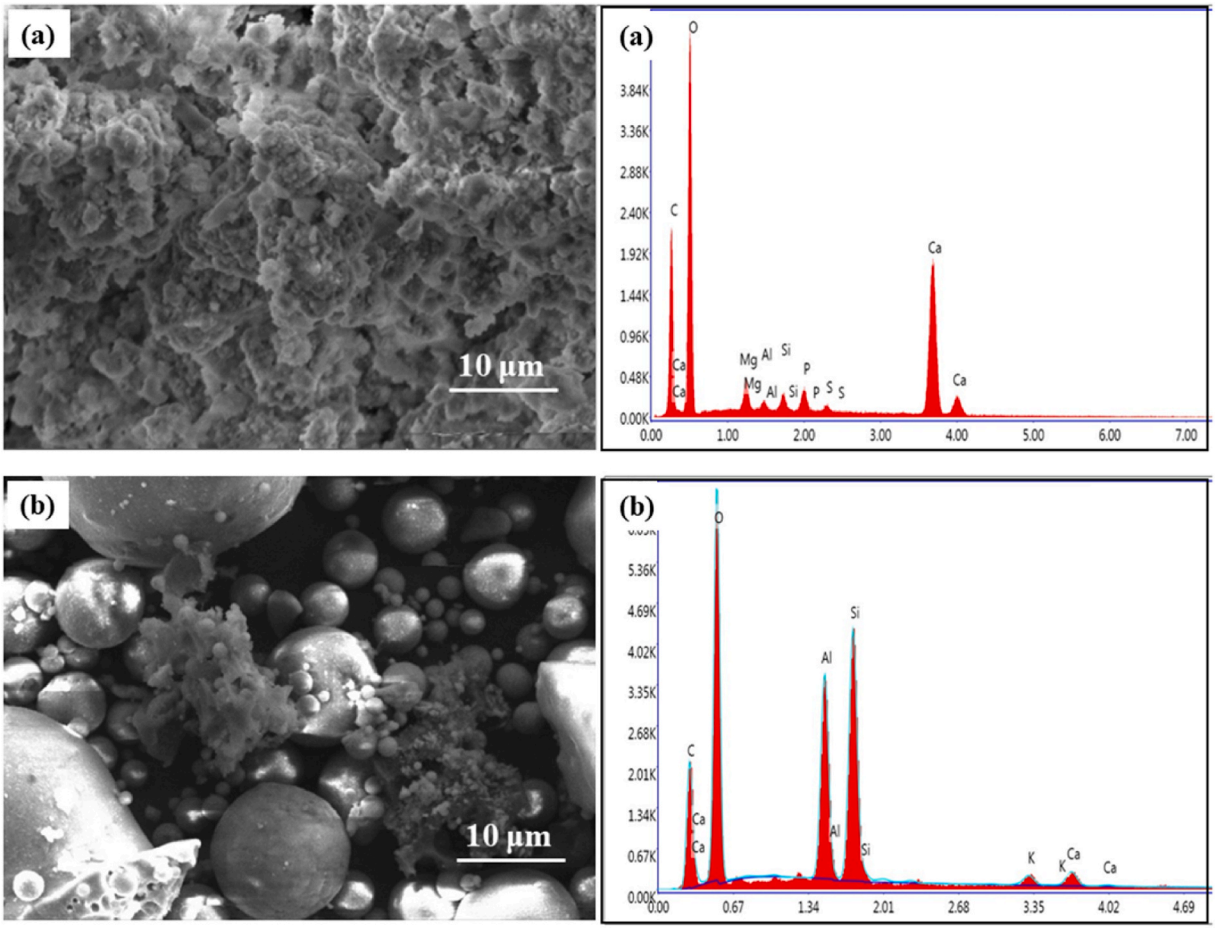

Fig. 3. SEM images and their corresponding EDX spectra of (a) sugar scum and (b) fly ash.

Table 3
Doehlert experimental plan and experimental results.

N° Exp.	T (°C)	τ (%)	T (min)	Y_1 (g/cm^3)	Y_2 (%)	Y_3 (MPa)
1	1200	10.00	240	2.15	33.14	37.54
2	1000	10.00	240	2.09	37.50	3.50
3	1150	18.66	240	2.12	41.75	9.69
4	1050	1.34	240	2.05	35.32	3.74
5	1150	1.34	240	2.14	25.82	12.70
6	1050	18.66	240	2.16	37.64	5.08
7	1150	12.89	338	2.15	34.45	12.99
8	1050	7.11	142	2.08	33.33	8.91
9	1150	7.11	142	2.13	33.50	3.19
10	1100	15.77	142	2.09	38.54	6.34
11	1050	12.89	338	2.12	38.16	8.84
12	1100	4.23	338	2.10	31.92	22.97
13	1100	10.00	240	2.08	39.44	10.90
14	1100	10.00	240	2.15	34.80	11.35
15	1100	10.00	240	2.10	32.37	13.65

and the amount of sugar scum causes a significant decrease in the compressive strength, as depicted in Fig. 4c. The best compressive strength is obtained with a low amount of sugar scum and during a long sintering time. For a sintering time over 240 min, the increase in the amount of sugar scum led to an augmentation in the porosity of the ceramic membrane, consequently decreasing its compressive strength.

Table 4
Estimated coefficients for responses Y_1, Y_2, and Y_3.

N.	Density Y_1		Porosity Y_2		Compressive strength Y_3	
	Coefficient	Signif. %	Coefficient	Signif. %	Coefficient	Signif. %
$\mathbf{b_0}$	2.110		35.537		11.967	
$\mathbf{b_1}$	0.031	4.79[a]	−2.206	11.2	10.010	0.538[b]
$\mathbf{b_2}$	0.022	12.1	5.324	0.561[b]	−2.060	10.8
$\mathbf{b_3}$	0.014	28.7	−0.171	88.7	5.381	1.83[a]
$\mathbf{b_{11}}$	0.010	66.7	−0.217	92.2	8.553	2.39[a]
$\mathbf{b_{22}}$	0.007	77.3	−0.467	83.2	−8.403	2.47[a]
$\mathbf{b_{33}}$	−0.002	93.9	−0.659	75.3	−2.177	23.0
$\mathbf{b_{12}}$	−0.075	4.22[a]	7.858	3.12[a]	−2.511	27.8
$\mathbf{b_{13}}$	0.014	66.4	−5.154	14.2	6.932	6.8
$\mathbf{b_{23}}$	0.034	32.0	−0.612	84.4	−14.724	1.63[a]

[a] Statistically significant at the level 95%.
[b] Statistically significant at the level 99%.

3.2.4. Optimization

The examination of the results of the response surfaces reveals that the responses Y_1, Y_2, and Y_3 exhibit distinct patterns of evolution and do not follow the same direction. Therefore, in order to prepare a competitive and efficient ceramic membrane with high density, porosity, and compressive strength, the optimization of sintering temperature, amount of sugar scum, and sintering time needs to be carried out simultaneously. This optimization process can be accomplished using the desirability function provided in the Nemrodw software. The desirability function operates within the range of [0,1], where a value of 1 represents the desired value, and 0 indicates an unsatisfactory response. The highest value of the desirability function signifies the most favorable overall combination of the responses Y_1, Y_2, and Y_3 within the experimental intervals of the investigated factors. This optimum corresponds to the most favorable experimental conditions. Table 5 presents the outcomes of the multi-criteria analysis.

The optimal point that maximizes the global function of desirability is achieved when using a temperature of sintering of 1197 °C, a sugar scum amount of 12.06 %, and a sintering time of 253 min. Under these conditions, the density, porosity, and compressive strength were calculated as 2.14 g/cm^3, 35.27 %, and 29.44 MPa, respectively. In order to validate the findings, three ceramic membrane samples were manufactured using the most favorable conditions. Under these conditions, the experimental values for density, porosity, and compressive strength were found to be 2.16 g/cm^3, 34.66%, and 28.24 MPa, respectively. The model exhibits excellent accuracy as the variance between the calculated and experimental values is below 1%.

3.3. Characterization of the optimum ceramic membrane

Fig. 5a illustrates the XRD spectra of the optimum ceramic membrane. According to JCPDS database numbers 96-900-0362, 96-900-1579, 96-900-6113, and 96-900-0362, the predominant crystal phases found in this membrane consist of anorthite, cristobalite, gehlenite, and mullite. The formation of the gehlenite phase, renowned for its pore-forming properties, contributes to the development of porosity in the produced ceramic membrane [33]. Suresh et al. [34] also noted the presence of mullite, gehlenite, and cristobalite phases in the anorthite-based ceramic membranes. At the optimal temperature, anorthite is formed when mullite and cristobalite combine with CaO present in the structure. Fly ash reacts with sugar scum to form anorthite according to the following equation (Eq. 10):

$$\frac{1}{x}(xAl_2O_3\ .\ ySiO_2\ )(\text{mullite}) + \left(2 - \frac{x}{y}\right)SiO_2\ + CaCO_3\ \rightarrow CaO.\ Al_2O_3.\ 2SiO_2 + CO_2 \qquad \text{Eq. 10}$$

The FTIR analysis, as illustrated in Fig. 5b, confirmed the results of the XRD analysis. The bands observed at approximately 1089, 930, 569, and 470 cm^{-1} can indeed demonstrate the presence of anorthite and mullite phases [31]. The band located at 1089 cm^{-1} was assigned to the stretching vibration of Si–O. The band at 930 cm^{-1} was attributed to Al–O stretching vibrations. The peak observed at 569 cm^{-1} was associated with the stretching vibration of the O–Si–O and Ca–O bonds present in the structure of anorthite [31]. The band located at 470 cm^{-1} resulted from the stretching vibration or internal bending of T-*O*-T (T = Si or Al) in the structure of aluminosilicate [31,35]. The peak observed at around 3446 cm^{-1} was related to the O–H stretching vibration of O–H. The peak at 1640 cm^{-1} was attributed to the water molecules bonded to the ceramic membrane's exchangeable cations [35].

Fig. 6a shows the SEM image of the membrane produced under the optimal conditions. It illustrates the porous morphology of the obtained membrane with diverse pore shapes and irregular distribution. The possible reason behind this nonuniformity may be the uneven distribution of the sugar scum in the membrane preparation mixture, which contains calcium carbonate as the primary phase. The decomposition of carbonates and the liberation of CO_2 create pores of various sizes. In light of this result, it can be deduced that this membrane has an appropriate morphology, qualifying it for use in wastewater treatment as a filtration membrane. As depicted in Fig. 6b, the primary constituents of the optimal ceramic membrane include oxygen (O), calcium (Ca), aluminum (Al), and silicon (Si). Fig. 7 depicts the variation in pore size of the optimal ceramic membrane, determined from SEM image using ImageJ software. The average pore size diameter varies between 0 and 4.5 μm. This result confirms that the pore size of the ceramic membrane was non-

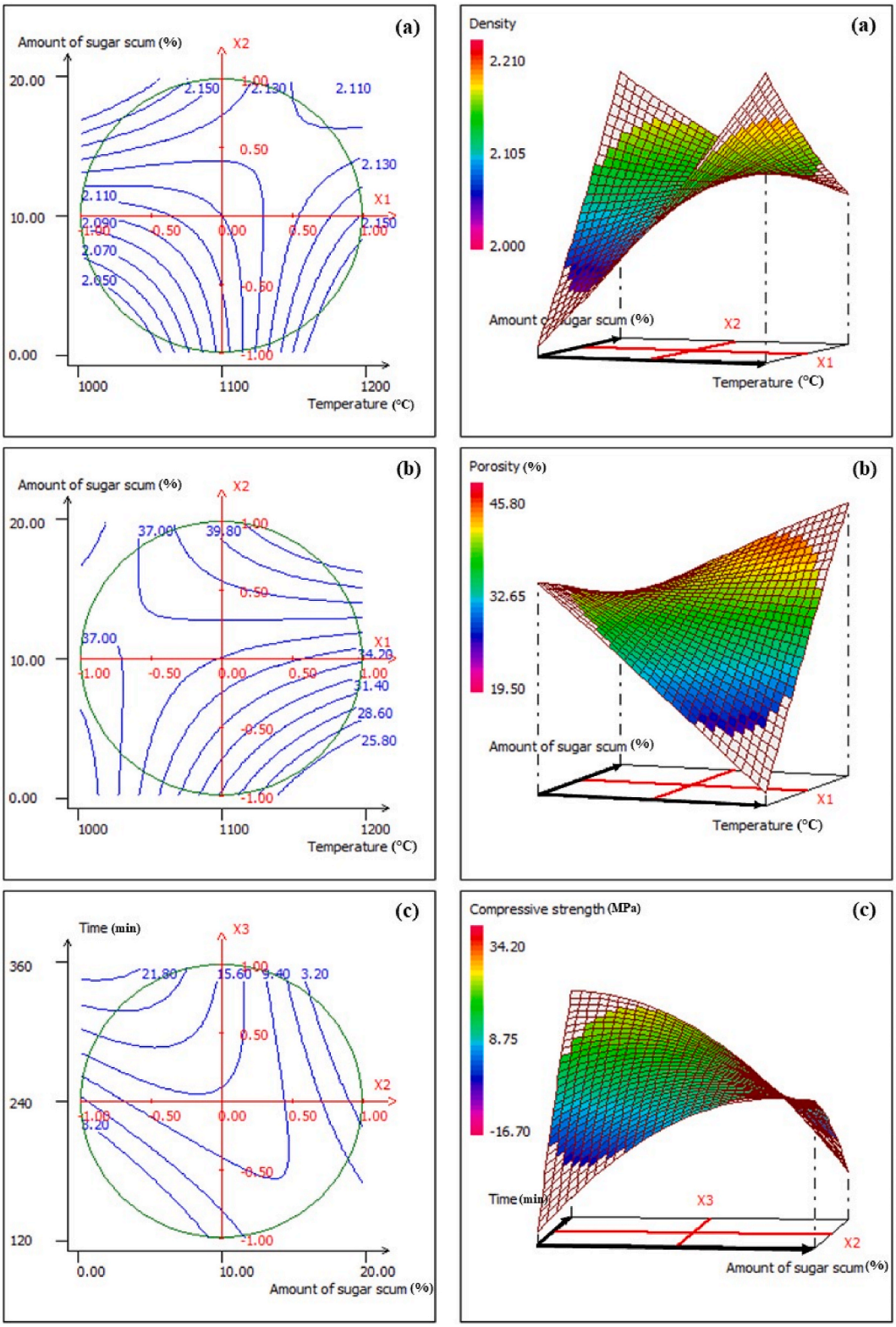

Fig. 4. Variation of the responses: (a) Y_1 as a function of temperature and amount of sugar scum, (b) Y_2 as a function of temperature and amount of sugar scum, and (c) Y_3 as a function of time and amount sugar scum.

Table 5
Characteristics of the maximum for Y1, Y2, and Y3.

Response	d_i %	$d_{i\ min}$ %	$d_{i\ max}$ %	$Y_{cal.}$	$Y_{exp.}$
Y_1: Density (g/cm^3)	84.91	63.11	100.00	2.14	2.16
Y_2: Porosity (%)	40.91	30.90	50.91	35.27	34.66
Y_3: Compressive strength (MPa)	37.03	29.41	44.65	29.44	28.24
Desirability	50.48	38.57	61.03		

d_i: partial desirability of response Y_i; $d_{i\ min}$: minimal partial desirability of response Y_i; $d_{i\ max}$: maximal partial desirability of response Y_i; Y_{cal}: calculated value; Y_{exp}.: experimental value.

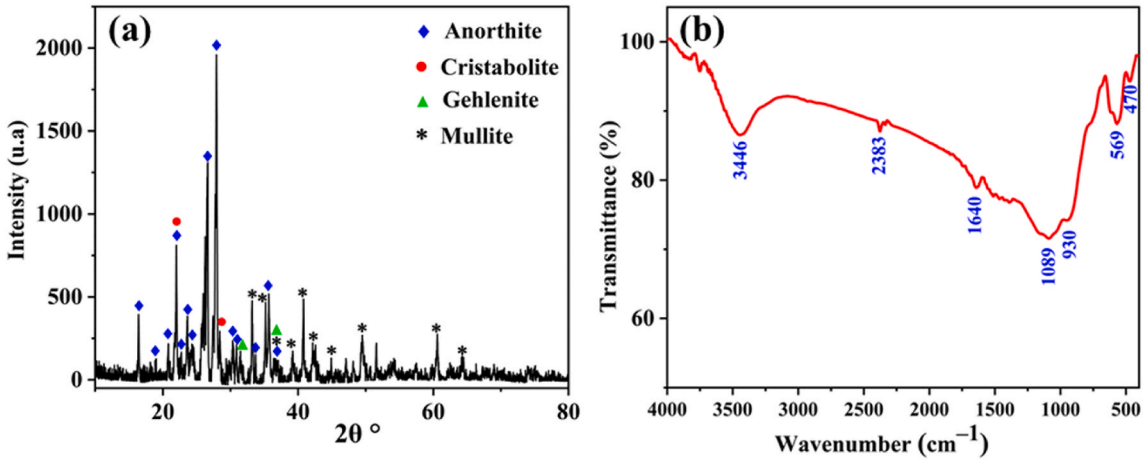

Fig. 5. (a) XRD patterns and (b) FTIR spectrum of the optimal ceramic membrane.

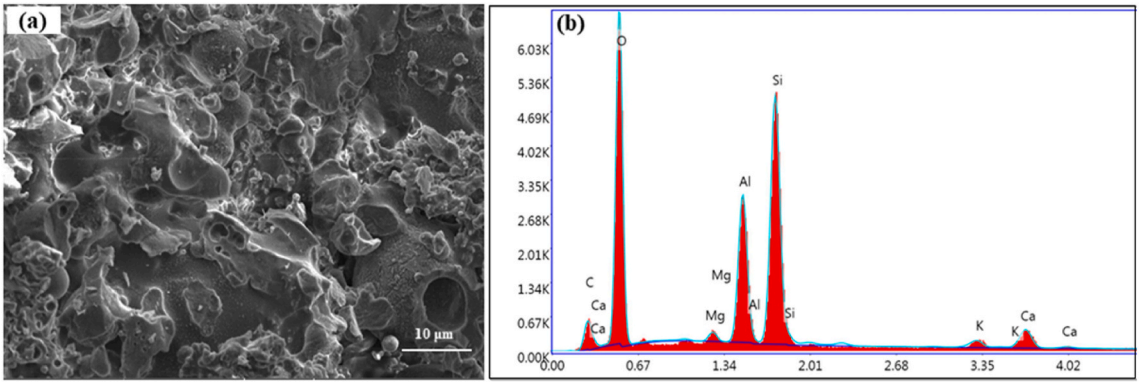

Fig. 6. (a) SEM image and b) its corresponding EDX spectrum of the optimal ceramic membrane.

uniform, which was consistent with the observation in Fig. 6.

The results of chemical stability tests, given in Fig. 8a, reveal that the membrane undergoes minimal weight loss in both acidic and basic mediums (less than 0.5 wt% in acidic medium and less than 0.1 wt% in basic medium), thus signifying the promising suitability of the membrane for use in harsh acidic and basic conditions. Indeed, the rate of mass loss is greater in acidic solution than in basic solution because the existence of CaO in the ceramic membrane is the primary factor leading to the reduction in the weight of the membrane after contacting acidic. The CaO present in the membrane reacts with hydrochloric acid, resulting in the formation of calcium chloride precipitates, which ultimately leads to a loss of weight [4].

The optimal ceramic membrane was evaluated by calculating its water permeability, which is an index to evaluate the membrane performance. For this purpose, the water fluxes were determined after 20 min of filtration for each transmembrane pressure. Fig. 8b presents the evolution of the water flux through the membrane versus the applied pressure. It is clear that Darcy's law is straightly respected and its slope, which corresponds to the permeability value, is approximately 2356.68 L/h m^2 bar. This result confirms that the obtained ceramic membrane is a promising candidate for wastewater treatment as a filtration membrane. The synthesized membrane offers excellent characteristics compared to other reported membranes (Table 6).

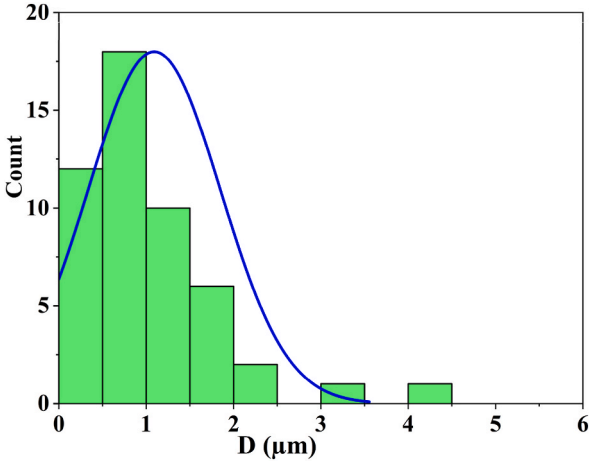

Fig. 7. Pore size distribution of the optimal ceramic membrane.

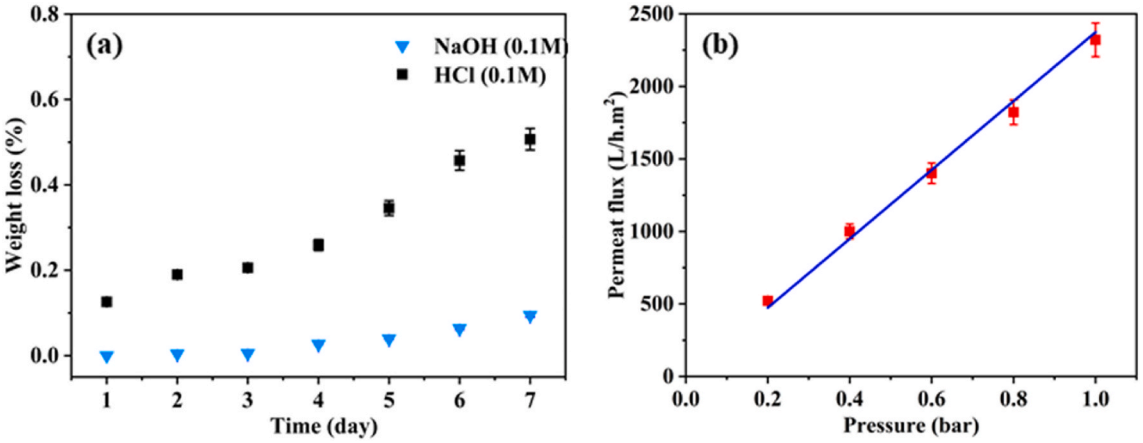

Fig. 8. (a) Mass loss in acidic and basic solution and (b) Water flux versus transmembrane pressure.

Table 6
Comparison of the characteristics of the synthesized membrane with the previously reported membranes.

Membrane	Porosity (%)	Compressive strength (MPa)	Permeability (L/h. m^2.bar)	Ref.
kaolin	40	25	53.64	[36]
natural clay and Moroccan phosphate	28.11	17.5	928	[37]
Kaolin, quartz and calcium carbonate	19.5	–	–	[38]
Kaolin; quartz	35–40	7–11	1600	[39]
Kaolin; alumina	18–41	13–38	900–3800	[40]
Kaolin; clay; feldspar; quartz; pirofilita	44	28	700–1800	[38]
Phosphate	–	–	700	[41]
Algerian kaolin	47	40	550	[42]
Kaolin; alumina; clay	36	39	410	[42]
Fly ash and sugar scum	34.66	28.24	2356.68	This study

3.4. Application to methylene blue solution

The efficiency of the optimized membrane was assessed by conducting filtration experiments with a MB solution having an initial concentration of 50 mg/L at a low pressure of 1 bar for the duration of 2 h of filtration. As shown in Fig. 9a, the permeate flux of MB dye decreased when increasing the filtration time. This decrease in flux could be attributed to the accumulation of MB dye on the surface of the membrane and/or the adsorption of MB dye within membrane pores [43]. Goswami et al. have also reported a decrease in permeate flux with increasing filtration time [4]. It is noteworthy that during the initial 40 min of treatment, the membrane displayed an impressive retention rate of 99.9 % for MB dye. In this context, Fig. 9b illustrates a photo comparison of the MB solution before and

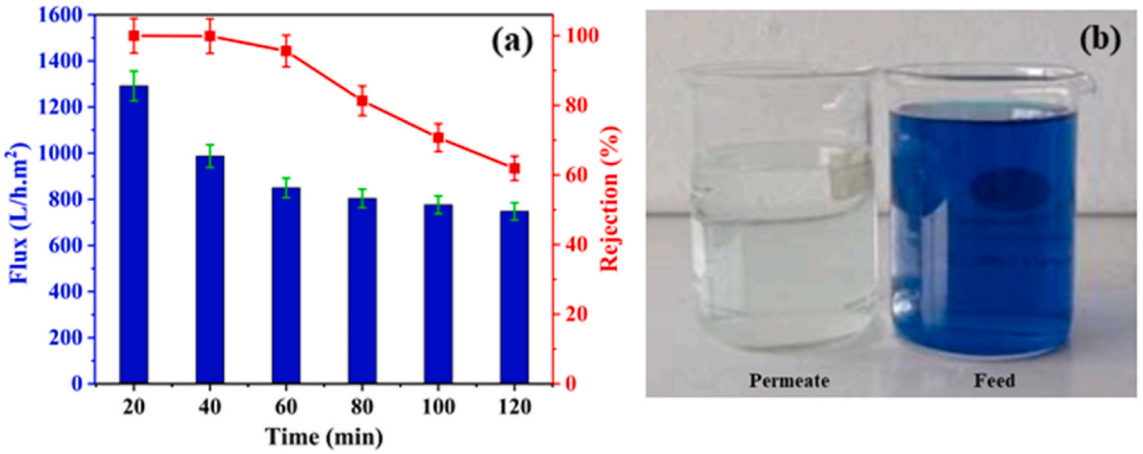

Fig. 9. (a) Evolution of flux versus filtration time and (b) Image comparison of feed and permeate samples.

after treatment by filtration through the prepared membrane, where a successful separation is clearly visible.

4. Conclusion

In this study, an anorthite-based ceramic membrane was prepared using fly ash and sugar scum as low-cost precursors and used as a membrane filter for MB removal from an aqueous solution. The optimum conditions for preparing a suitable membrane with high density, porosity, and compressive strength were determined using the experimental design methodology and determined to be at a temperature of 1197 °C, with an amount of sugar scum of 12.06 %, and a sintering time of 253 min. Under these conditions, the ceramic membrane exhibited a density of 2.16 g/cm^3, porosity of 34.66 %, and compressive strength of 28.24 MPa. The obtained membrane demonstrated high permeability and excellent chemical resistance in both acidic and alkaline environments. The filtration efficacy of the prepared membrane was assessed in a simplified medium, revealing a high retention rate for MB dye. These preliminary findings are encouraging, suggesting that this material could have important applications in treating industrial effluents. As a perspective, it would be beneficial to evaluate this membrane using industrial effluents. Such evaluations would offer valuable insights into its performance in real-world conditions, verifying its efficacy in practical applications for contaminant mitigation.

Data availability statement

No data was used for the research described in the article.

CRediT authorship contribution statement

Y. El Maguana: Writing – review & editing, Writing – original draft, Visualization, Data curation, Conceptualization. **R. Chikri:** Visualization. **K. Elataoui:** Visualization, Validation. **H. Ait Said:** Visualization, Validation. **M. Benchanaa:** Visualization, Validation, Supervision. **N. Elhadiri:** Visualization, Validation, Supervision.

Declaration of competing interest

The authors declare that they have no known competing financial interests or personal relationships that could have appeared to influence the work reported in this paper.

Acknowledgments

The authors express their gratitude to the Center of Analyses and Characterization (CAC) at the University Caddy Ayyad, Morocco. We also express our gratitude to those who supported, participated in, and contributed to this study, making it possible.

References

[1] Y. El maguana, N. Elhadiri, M. Benchanaa, R. Chikri, R. Idouhli, K. Tabit, Low-cost and high-performance ceramic membrane from sugar industry waste: characterization and optimization using experimental design, Mater. Today Proc. 53 (2022) 310–317, https://doi.org/10.1016/j.matpr.2022.02.208.
[2] R. Chikri, N. Elhadiri, M. Benchanaa, Y. El maguana, Two-step optimization of the preparation conditions of a high-quality activated carbon derived from sawdust, Biomass Convers. Biorefinery (2023) 9–14, https://doi.org/10.1007/s13399-023-03965-9.
[3] W. Misrar, M. Loutou, L. Saadi, M. Mansori, M. Waqif, C. Favotto, Cordierite containing ceramic membranes from smectetic clay using natural organic wastes as pore-forming agents, J. Asian Ceram. Soc. 5 (2017) 199–208, https://doi.org/10.1016/j.jascer.2017.04.007.

[4] K.P. Goswami, G. Pugazhenthi, Effect of binder concentration on properties of low-cost fly ash-based tubular ceramic membrane and its application in separation of glycerol from biodiesel, J. Clean. Prod. 319 (2021) 128679, https://doi.org/10.1016/j.jclepro.2021.128679.
[5] F. Galliou, N. Markakis, M.S. Fountoulakis, N. Nikolaidis, T. Manios, Production of organic fertilizer from olive mill wastewater by combining solar greenhouse drying and composting, Waste Manag. 75 (2018) 305–311, https://doi.org/10.1016/j.wasman.2018.01.020.
[6] Y. Van Fan, J.J. Klemeš, C.T. Lee, S. Perry, Anaerobic digestion of municipal solid waste: energy and carbon emission footprint, J. Environ. Manage. 223 (2018) 888–897, https://doi.org/10.1016/j.jenvman.2018.07.005.
[7] J. Usman, M.H.D. Othman, A.F. Ismail, M. A Rahman, J. Jaafar, T. Abdullahi, Comparative study of Malaysian and Nigerian kaolin-based ceramic hollow fiber membranes for filtration application, Malaysian J. Fundam. Appl. Sci. 16 (2020) 182–185, https://doi.org/10.11113/mjfas.v16n2.1484.
[8] M.B. Asif, Z. Zhang, Ceramic membrane technology for water and wastewater treatment: a critical review of performance, full-scale applications, membrane fouling and prospects, Chem. Eng. J. 418 (2021) 129481, https://doi.org/10.1016/j.cej.2021.129481.
[9] J. Usman, M.H.D. Othman, A.F. Ismail, M.A. Rahman, J. Jaafar, Y.O. Raji, A.O. Gbadamosi, T.H. El Badawy, K.A.M. Said, An overview of superhydrophobic ceramic membrane surface modification for oil-water separation, J. Mater. Res. Technol. 12 (2021) 643–667, https://doi.org/10.1016/j.jmrt.2021.02.068.
[10] J. Usman, N. Baig, I.H. Aljundi, Superhydrophilic and underwater superoleophobic ceramic membranes grafted by layered polydopamine and polydopamine encapsulated silica particles for efficient separation of oil-in-water emulsions, J. Environ. Chem. Eng. 11 (2023) 110011, https://doi.org/10.1016/j.jece.2023.110011.
[11] L. Treccani, T. Yvonne Klein, F. Meder, K. Pardun, K. Rezwan, Functionalized ceramics for biomedical, biotechnological and environmental applications, Acta Biomater. 9 (2013) 7115–7150, https://doi.org/10.1016/j.actbio.2013.03.036.
[12] H. Wu, X. Xu, L. Shi, Y. Yin, L.-C. Zhang, Z. Wu, X. Duan, S. Wang, H. Sun, Manganese oxide integrated catalytic ceramic membrane for degradation of organic pollutants using sulfate radicals, Water Res. 167 (2019) 115110, https://doi.org/10.1016/j.watres.2019.115110.
[13] M. Issaoui, L. Limousy, Low-cost ceramic membranes: synthesis, classifications, and applications, Comptes Rendus Chim 22 (2019) 175–187, https://doi.org/10.1016/j.crci.2018.09.014.
[14] A. Kayvani Fard, G. McKay, A. Buekenhoudt, H. Al Sulaiti, F. Motmans, M. Khraisheh, M. Atieh, Inorganic membranes: preparation and application for water treatment and desalination, Materials 11 (2018) 74, https://doi.org/10.3390/ma11010074.
[15] S.L. Sandhya Rani, R.V. Kumar, Insights on applications of low-cost ceramic membranes in wastewater treatment: a mini-review, Case Stud. Chem. Environ. Eng. 4 (2021) 100149, https://doi.org/10.1016/j.cscee.2021.100149.
[16] S.A. Alftessi, M.H.D. Othman, M.R. Adam, T.M. Farag, A.F. Ismail, M.A. Rahman, J. Jaafar, M.A. Habib, Y.O. Raji, S.K. Hubadillah, Novel silica sand hollow fibre ceramic membrane for oily wastewater treatment, J. Environ. Chem. Eng. 9 (2021) 104975, https://doi.org/10.1016/j.jece.2020.104975.
[17] A. Khalfaoui, M. Hajjaji, S. Kacim, A. Bacaoui, Evaluation of the simultaneous effects of firing cycle parameters on technological properties and ceramic suitability of a raw clay using the response surface methodology, J. Am. Ceram. Soc. 89 (2006) 1563–1567, https://doi.org/10.1111/j.1551-2916.2006.00955.x.
[18] X. Wang, K. Sun, G. Zhang, F. Yang, S. Lin, Y. Dong, Robust zirconia ceramic membrane with exceptional performance for purifying nano-emulsion oily wastewater, Water Res. 208 (2022) 117859, https://doi.org/10.1016/j.watres.2021.117859.
[19] W. Zhu, Y. Liu, K. Guan, C. Peng, W. Qiu, J. Wu, Integrated preparation of alumina microfiltration membrane with super permeability and high selectivity, J. Eur. Ceram. Soc. 39 (2019) 1316–1323, https://doi.org/10.1016/j.jeurceramsoc.2018.10.022.
[20] J. Fang, G. Qin, W. Wei, X. Zhao, L. Jiang, Elaboration of new ceramic membrane from spherical fly ash for microfiltration of rigid particle suspension and oil-in-water emulsion, Desalination 311 (2013) 113–126, https://doi.org/10.1016/j.desal.2012.11.008.
[21] S. Saja, A. Bouazizi, B. Achiou, M. Ouammou, A. Albizane, J. Bennazha, S.A. Younssi, Elaboration and characterization of low-cost ceramic membrane made from natural Moroccan perlite for treatment of industrial wastewater, J. Environ. Chem. Eng. 6 (2018) 451–458, https://doi.org/10.1016/j.jece.2017.12.004.
[22] A. Agarwalla, K. Mohanty, Comprehensive characterization, development, and application of natural/Assam Kaolin-based ceramic microfiltration membrane, Mater. Today Chem. 23 (2022) 100649, https://doi.org/10.1016/j.mtchem.2021.100649.
[23] A. Belgada, B. Achiou, S. Alami Younssi, F.Z. Charik, M. Ouammou, J.A. Cody, R. Benhida, K. Khaless, Low-cost ceramic microfiltration membrane made from natural phosphate for pretreatment of raw seawater for desalination, J. Eur. Ceram. Soc. 41 (2021) 1613–1621, https://doi.org/10.1016/j.jeurceramsoc.2020.09.064.
[24] A. Manni, B. Achiou, A. Karim, A. Harrati, C. Sadik, M. Ouammou, S. Alami Younssi, A. El Bouari, New low-cost ceramic microfiltration membrane made from natural magnesite for industrial wastewater treatment, J. Environ. Chem. Eng. 8 (2020) 103906, https://doi.org/10.1016/j.jece.2020.103906.
[25] A. Bouazizi, S. Saja, B. Achiou, M. Ouammou, J.I. Calvo, A. Aaddane, S.A. Younssi, Elaboration and characterization of a new flat ceramic MF membrane made from natural Moroccan bentonite. Application to treatment of industrial wastewater, Appl. Clay Sci. (2016) 132–133, https://doi.org/10.1016/j.clay.2016.05.009, 33–40.
[26] B. Achiou, H. Elomari, A. Bouazizi, A. Karim, M. Ouammou, A. Albizane, J. Bennazha, S. Alami Younssi, I.E. El Amrani, Manufacturing of tubular ceramic microfiltration membrane based on natural pozzolan for pretreatment of seawater desalination, Desalination 419 (2017) 181–187, https://doi.org/10.1016/j.desal.2017.06.014.
[27] A. Agarwal, A. Samanta, B.K. Nandi, A. Mandal, Synthesis, characterization and performance studies of kaolin-fly ash-based membranes for microfiltration of oily waste water, J. Pet. Sci. Eng. 194 (2020) 107475, https://doi.org/10.1016/j.petrol.2020.107475.
[28] K. Tabit, H. Hajjou, M. Waqif, L. Saâdi, Cordierite-based ceramics from coal fly ash for thermal and electrical insulations, Silicon 13 (2021) 327–334, https://doi.org/10.1007/s12633-020-00428-y.
[29] M. Loutou, M. Hajjaji, M.A. Babram, M. Mansori, C. Favotto, R. Hakkou, Phosphate sludge-based ceramics: microstructure and effects of processing factors, J. Build. Eng. 11 (2017) 48–55, https://doi.org/10.1016/j.jobe.2017.04.002.
[30] H.A. Said, I. Ait Bourhim, A. Ouarga, I. Iraola-Arregui, M. Lahcini, A. Barroug, H. Noukrati, H. Ben youcef, Sustainable phosphorylated microcrystalline cellulose toward enhanced removal performance of methylene blue, Int. J. Biol. Macromol. 225 (2023) 1107–1118, https://doi.org/10.1016/j.ijbiomac.2022.11.172.
[31] K. Tabit, M. Waqif, L. Saâdi, Anorthite-cordierite based binary ceramics from coal fly ash and steel slag for thermal and dielectric applications, Mater. Chem. Phys. 254 (2020) 123472, https://doi.org/10.1016/j.matchemphys.2020.123472.
[32] Y. El maguana, N. Elhadiri, M. Bouchdoug, M. Benchanaa, A. Boussetta, Optimization of preparation conditions of novel adsorbent from sugar scum using response surface methodology for removal of methylene blue, J. Chem. 2018 (2018) 1–10, https://doi.org/10.1155/2018/2093654.
[33] M. Loutou, W. Misrar, M. Koudad, M. Mansori, L. Grase, C. Favotto, Y. Taha, R. Hakkou, Phosphate mine tailing recycling in membrane filter manufacturing: microstructure and filtration suitability, Minerals 9 (2019) 318, https://doi.org/10.3390/min9050318.
[34] K. Suresh, G. Pugazhenthi, R. Uppaluri, Fly ash based ceramic microfiltration membranes for oil-water emulsion treatment: parametric optimization using response surface methodology, J. Water Process Eng. 13 (2016) 27–43, https://doi.org/10.1016/j.jwpe.2016.07.008.
[35] L. Wu, C. Li, H. Li, H. Wang, W. Yu, K. Chen, X. Zhang, Preparation and characteristics of porous anorthite ceramics with high porosity and high-temperature strength, Int. J. Appl. Ceram. Technol. 17 (2020) 963–973, https://doi.org/10.1111/ijac.13430.
[36] M. Purnima, T. Paul, K. Pakshirajan, G. Pugazhenthi, Onshore oilfield produced water treatment by hybrid microfiltration-biological process using kaolin based ceramic membrane and oleaginous Rhodococcus opacus, Chem. Eng. J. 453 (2023) 139850.
[37] M. Mouiya, A. Abourriche, A. Bouazizi, A. Benhammou, Y. El Hafiane, Y. Abouliatim, L. Nibou, M. Oumam, M. Ouammou, A. Smith, Flat ceramic microfiltration membrane based on natural clay and Moroccan phosphate for desalination and industrial wastewater treatment, Desalination 427 (2018) 42–50.
[38] M. Latwal, S. Arora, A. Joshi, M. Irfan, G. Pandey, Sustainable ceramic membrane for decontamination of water: a cost-effective approach, Heliyon 9 (2023) e13321, https://doi.org/10.1016/j.heliyon.2023.e13321.
[39] S. Emani, R. Uppaluri, M.K. Purkait, Preparation and characterization of low cost ceramic membranes for mosambi juice clarification, Desalination 317 (2013) 32–40, https://doi.org/10.1016/j.desal.2013.02.024.
[40] I. Hedfi, N. Hamdi, M.A. Rodriguez, E. Srasra, Development of a low cost micro-porous ceramic membrane from kaolin and Alumina, using the lignite as porogen agent, Ceram. Int. 42 (2016) 5089–5093, https://doi.org/10.1016/j.ceramint.2015.12.023.

[41] I. Barrouk, S. Alami Younssi, A. Kabbabi, M. Persin, A. Albizane, S. Tahiri, New ceramic membranes from natural Moroccan phosphate for microfiltration application, Desalin. Water Treat. 55 (2015) 53–60.
[42] B. Ghouil, A. Harabi, F. Bouzerara, B. Boudaira, A. Guechi, M.M. Demir, A. Figoli, Development and characterization of tubular composite ceramic membranes using natural alumino-silicates for microfiltration applications, Mater. Charact. 103 (2015) 18–27, https://doi.org/10.1016/j.matchar.2015.03.009.
[43] S. Saja, A. Bouazizi, B. Achiou, H. Ouaddari, A. Karim, M. Ouammou, A. Aaddane, J. Bennazha, S. Alami Younssi, Fabrication of low-cost ceramic ultrafiltration membrane made from bentonite clay and its application for soluble dyes removal, J. Eur. Ceram. Soc. 40 (2020) 2453–2462, https://doi.org/10.1016/j.jeurceramsoc.2020.01.057.